

Preparation, characterization, DFT calculations and ethylene oligomerization studies of iron(II) complexes bearing 2-(1H-benzimidazol-2-yl)-phenol derivatives

Marzieh Haghverdi, Azadeh Tadjarodi, Naeimeh Bahri-Laleh & Mehdi Nekoomanesh Haghighi

To cite this article: Marzieh Haghverdi, Azadeh Tadjarodi, Naeimeh Bahri-Laleh & Mehdi Nekoomanesh Haghighi (2018): Preparation, characterization, DFT calculations and ethylene oligomerization studies of iron(II) complexes bearing 2-(1H-benzimidazol-2-yl)-phenol derivatives, Journal of Coordination Chemistry, DOI: [10.1080/00958972.2018.1446527](https://doi.org/10.1080/00958972.2018.1446527)

To link to this article: <https://doi.org/10.1080/00958972.2018.1446527>

 View supplementary material 

 Accepted author version posted online: 28 Feb 2018.

 Submit your article to this journal 

 View related articles 

 View Crossmark data 

Publisher: Taylor & Francis

Journal: *Journal of Coordination Chemistry*

DOI: <http://doi.org/10.1080/00958972.2018.1446527>



Preparation, characterization, DFT calculations and ethylene oligomerization studies of iron(II) complexes bearing 2-(1H-benzimidazol-2-yl)-phenol derivatives

MARZIEH HAGHVERDI[†], AZADEH TADJARODI^{*†}, NAEIMEH BAHRI-LALEH[‡] and MEHDI NEKOOMANESH HAGHIGHI[‡]

[†]Research Laboratory of Inorganic Materials Synthesis, Department of Chemistry, Iran University of Science and Technology, Tehran, Iran

[‡]Polymerization Engineering Department, Iran Polymer and Petrochemical Institute (IPPI), Tehran, Iran

Five 2-(1*H*-benzimidazol-2-yl)-phenol derivatives including 1H (HL₁), 5-chloro- (HL₂), 5-methyl- (HL₃), 5,6-dichloro- (HL₄) and 5,6-dimethyl- (HL₅) were synthesized by the reaction of their corresponding benzene-1,2-diamine precursors and 2-hydroxybenzaldehyde which subsequently was employed in complexation with Fe(II) to prepare complexes **C1-C5**, respectively. Indeed, in all complexes, the ligands were coordinated as bidentate, *via* the C=N nitrogen and hydroxy oxygen atom of benzimidazole moiety and phenol ring, respectively. The compounds were characterized by FT-IR, UV-vis, ¹H- and ¹³C-NMR spectroscopy, ICP and elemental analysis (C, H and N). The purity of these compounds was determined by melting point (m.p) (and TLC). The synthesized ligands and complexes were geometrically optimized by Gaussian09 software at B3LYP/TZVP level of theory and satisfactory theoretical-experimental agreement was achieved for analysis of IR data of the compounds. Catalytic behavior of the iron(II) complexes was investigated for ethylene reactivity. On activation with diethylaluminum chloride (Et₂AlCl), iron(II) complex (**C4**) showed the highest activity (1686 kg oligomers.mol⁻¹(Fe).h⁻¹) for ethylene oligomerization when it contains chlorine substituents and exhibits good selectivity for linear 1-butene. The steric and electronic effects of ligands were investigated in detail on the influence of their catalytic activities.

Keywords: Benzimidazolyl-phenols; Iron(II) complexes; DFT Calculations; Ethylene oligomerization; Substituent effects

^{*}Corresponding author. Email: tajarodi@iust.ac.ir

1. Introduction

Ethylene oligomerization is a major industrial process for producing linear α -olefins, about six millions of tons productivities annually, which provide basic feedstocks in the preparation of detergents, synthetic lubricants, plasticizers, alcohols and comonomers used for branched polyolefins [1]. The iron and cobalt catalysts showed unique properties for high selectivity of vinyl type oligomers and polyolefins (polyolefin waxes) produced, which was initially found by research groups of Brookhart and Gibson using bis(imino)pyridyl iron and cobalt complexes [2-4]. In the recent decade, the intensive researches have explored numerous model complexes of late-transition metals as catalysts toward ethylene reactivity [5, 6]. However, a few models of iron catalysts showed good catalytic activities toward ethylene oligomerization and polymerization in comparison with various models of late-transition metals complexes. Nevertheless, there are some significant advantages for iron catalysts, such as high catalytic activity, high α -olefin selectivity in ethylene oligomerization, and lower toxicity than other metals [7]. Therefore, relative research works have been focused on new models of iron complexes are still highly attractive, and the comprehensive review papers are reported. Alternative models of iron complex catalysts bearing bi- and tri-dentate ligands for ethylene reactivity have been intensively explored [8-11]. There are reports about the use of benzimidazolyl-phenol and its derivatives in the role of bidentate ligands with different transition metals. Given the easy preparation, good stability and rich coordination chemistry of these ligands, the synthesis of their transition metal complexes has been deeply explored [12]. Metal complexes with these ligands are important because of their high thermal stability, good catalytic performance and superior optical properties [13].

Herein, we discuss our investigations on the synthesis and characterization of Fe(II) complexes having 2-(1*H*-benzimidazol-2-yl)-phenol derivatives as ligands. The optimized geometry and vibrational frequency calculations of these compounds were derived from theoretical calculation in B3LYP/TZVP level on Gaussian09 program. Also, the catalytic behavior of Fe(II) complexes in ethylene reactivity was investigated. They showed good catalytic activities toward ethylene oligomerization in the presence of diethylaluminum chloride (Et_2AlCl). The relationship between the structures of the complexes, their catalytic activities and product properties are discussed in detail.

2. Experimental

2.1. General methods and materials

All manipulations of air- and moisture-sensitive compounds were carried out under nitrogen using standard Schlenk techniques. Toluene was refluxed over sodium-benzophenone and distilled under nitrogen prior to use. Diethylaluminum chloride (Et_2AlCl) was purchased from Aldrich Chemicals. All other chemicals were obtained commercially and used without purification. Elemental analyses were performed on a Perkin Elmer model 2400 series 2 (made in USA) automatic carbon, hydrogen, nitrogen analyzer. Determination of metal percent was performed using ICP (3410ARL model made in Swiss). NMR spectra (300 MHz for ^1H and 75 MHz for ^{13}C) were measured with a Bruker AVANCE-300 instrument (made in Germany) in dimethylsulfoxide (DMSO-d_6) using tetramethylsilane (TMS) as internal standard. IR spectra were recorded in KBr disks on a Shimadzu FT-IR 8400 spectrometer (made in Japan) from 400-4000 cm^{-1} . UV-vis absorption spectra were recorded using a Shimadzu, UV-1700 spectrophotometer (made in Japan) in DMSO solution. GC analyses were performed with a Varian CP-3800 gas chromatograph equipped with a flame ionization detector and a 100 m (0.25 mm i.d., 0.5 μm film thickness) CP-Sil PONA CB. The yield of oligomers was calculated by referencing with the mass of the solvent on the basis of the prerequisite that the mass of each fraction was approximately proportional to its integrated areas in the GC trace. Selectivity for linear 1-alkenes was defined as (amount of linear 1-alkenes of all fractions)/(total amount of oligomer products) in percentage. Melting points were determined using an electrothermal melting point apparatus.

2.2. Synthesis of the ligands: General procedure

The ligands (five 2-(1H-benzimidazol-2-yl)-phenol derivatives including 1H- (HL_1), 5-chloro- (HL_2), 5-methyl- (HL_3), 5,6-dichloro- (HL_4) and 5,6-dimethyl- (HL_5)) were prepared according to our previous literature procedures [14]. For instance, 2-(5,6-dichloro-1H-benzimidazol-2-yl)-phenol (HL_4) was synthesized by reacting 2-hydroxybenzaldehyde (1.83 g, 15.0 mmol) with an equivalent amount of sodium metabisulfide (1.60 g, 8.5 mmol) at room temperature in EtOH (20 mL) for several minutes. The reaction mixture was stirred vigorously and 10 mL ethanol was added. The mixture was kept in a refrigerator overnight. The mixture was treated with

4,5-dichlorobenzene-1,2-diamine (0.71 g, 4.0 mmol) in 10 mL dimethylformamide (DMF) and was gently refluxed for 4 h. The completion of reaction was checked by TLC. Then the reaction mixture was poured into 100 mL icy water, filtered and crystallized from ethanol. This method was selected because of its ease, high yield and short synthesis time. This obtained ligand was used for the synthesis of complex **C4**. Molecular structure of the synthesized ligands is given in scheme 1.

2.3. Synthesis of complexes C1-C5

Complexes **C1-C5** were synthesized by the reaction of $\text{FeCl}_2 \cdot 4\text{H}_2\text{O}$ (0.049 g, 0.25 mmol) with the corresponding ligands and KOH (0.028 g, 0.5 mmol) in methanol. A typical synthetic procedure for **C1** can be described as follows: the ligand HL_1 (0.106 g, 0.5 mmol), KOH (0.028 g, 0.5 mmol) and $\text{FeCl}_2 \cdot 4\text{H}_2\text{O}$ (0.049 g, 0.25 mmol) were added to a Schlenk tube, followed by the addition of freshly distilled methanol (15 mL) with rapid stirring at room temperature. The color of solution changed immediately. The completion of reaction was monitored by TLC. The reaction mixture was stirred for 24 h, and then the precipitate was washed with diethylether several times and dried to give the pure product as a brown-orange powder in 69% yield. FT-IR (KBr disc, cm^{-1}), 3415 $\nu(\text{N-H})$, 3184 $\nu(\text{C-H})$, 1623 $\nu(\text{C=N})$, 1531 $\nu(\text{C=C})$, 1259 $\nu(\text{C-O})$, 472, 549 $\nu(\text{Fe-O})$, 426 $\nu(\text{Fe-N})$. Anal. Calcd. for $\text{C}_{26}\text{H}_{26}\text{N}_4\text{O}_6\text{K}_2\text{Cl}_2\text{Fe}$: C, 45.00; H, 3.74; N, 8.05; Fe, 8.03. Found: C, 45.09; H, 4.02; N, 8.47; Fe, 7.86 %. UV-vis (DMSO, nm), 510.

Data for **C2** are as follows: Brown-orange powder, yield: 51%, FT-IR (KBr disc, cm^{-1}), 3417 $\nu(\text{N-H})$, 3174 $\nu(\text{C-H})$, 1628 $\nu(\text{C=N})$, 1558 $\nu(\text{C=C})$, 1257 $\nu(\text{C-O})$, 470, 534 $\nu(\text{Fe-O})$, 424 $\nu(\text{Fe-N})$. Anal. Calcd. for $\text{C}_{26}\text{H}_{18}\text{N}_4\text{O}_3\text{K}_2\text{Cl}_4\text{Fe}$: C, 43.95; H, 2.53; N, 7.88; Fe, 7.86. Found: C, 43.87; H, 2.43; N, 7.52; Fe, 7.90 %. UV-vis (DMSO, nm), 480.

Data for **C3** are as follows: Brown-orange powder, yield: 59%, FT-IR (KBr disc, cm^{-1}), 3421 $\nu(\text{N-H})$, 3058 $\nu(\text{C-H})$, 1631 $\nu(\text{C=N})$, 1558 $\nu(\text{C=C})$, 1261 $\nu(\text{C-O})$, 486, 578 $\nu(\text{Fe-O})$, 418 $\nu(\text{Fe-N})$. Anal. Calcd. for $\text{C}_{28}\text{H}_{22}\text{N}_4\text{O}_2\text{K}_2\text{Cl}_2\text{Fe}$: C, 51.62; H, 3.38; N, 8.60; Fe, 8.57. Found: C, 51.24; H, 3.00; N, 8.86; Fe, 8.87 %. UV-vis (DMSO, nm), 500.

Data for **C4** are as follows: Black grey powder, yield: 57%, FT-IR (KBr disc, cm^{-1}), 3419 $\nu(\text{N-H})$, 3112 $\nu(\text{C-H})$, 1623 $\nu(\text{C=N})$, 1558 $\nu(\text{C=C})$, 1257 $\nu(\text{C-O})$, 461, 520 $\nu(\text{Fe-O})$, 426 $\nu(\text{Fe-N})$.

Anal. Calcd. for $C_{26}H_{14}N_4O_2Cl_4Fe$: C, 50.99; H, 2.28; N, 9.15; Fe, 9.12. Found: C, 50.33; H, 2.06; N, 8.96; Fe, 9.82 %. UV-vis (DMSO, nm), 510.

Data for **C5** are as follows: Black grey powder, yield: 50%, FT-IR (KBr disc, cm^{-1}), 3406 $\nu(N-H)$, 3058 $\nu(C-H)$, 1631 $\nu(C=N)$, 1560 $\nu(C=C)$, 1259 $\nu(C-O)$, 436, 516 $\nu(Fe-O)$, 409 $\nu(Fe-N)$.

Anal. Calcd. for $C_{32}H_{34}N_4O_4K_2Cl_2Fe$: C, 51.69; H, 4.57; N, 7.53; Fe, 7.51. Found: C, 51.17; H, 4.02; N, 7.72; Fe, 7.15 %. UV-vis (DMSO, nm), 504.

2.4. Computational details

All structures have been optimized with density functional theory (DFT) method using the B3LYP (hybrid GGA functional of Becke-Lee, Parr, and Yang [15, 16]) functional and triple- ζ valence TZVP [17] basis set, since as reported before, better agreement with the experimental results can be obtained with B3LYP and it is a widely used functional in the molecular simulation of transition metal catalytic systems [18-22]. All the calculations have been carried out with the Gaussian09 package [23].

For all the computed complexes, the quintet, containing four unpaired electrons, was the electronic ground state and thus open shell calculations were performed [23]. In order to ensure that the optimized geometries represent the global minima and that there are only positive eigenvalues, the vibrational frequency calculations were performed [24, 25]. The optimized geometry of compounds furnished the total energy E.

The energy values obtained by using the DFT calculations are: HL₁ (-686), HL₂ (-1146), HL₃ (-726), HL₄ (-1606), HL₅ (-765), **C1** (-3556), **C2** (-4475), **C3** (-3635), **C4** (-4474) and **C5** (-3713). Values inside parentheses are in a.u.

2.5. General procedure for ethylene oligomerization

Ethylene oligomerization was done in a 1-L autoclave stainless steel reactor equipped with a mechanical stirrer and a temperature controller. At first, reactor charged with toluene, the desired amount of cocatalyst, and toluene solution of catalytic precursor under a nitrogen atmosphere, the total volume was 110 mL. At the reaction temperature, the reactor was sealed and pressurized to 20 atm of ethylene pressure, and the ethylene pressure was kept with feeding of ethylene. After the reaction was carried out for the required time, the pressure was released and a small amount of the reaction solution was collected and then analyzed by gas chromatography (GC) for

determining the composition and mass distribution of oligomers obtained. Then the residual reaction solution was quenched with 5% hydrochloric acid ethanol in order to collect polyethylene obtained. However, the polyethylene was not formed.

3. Results and discussion

1*H*-Benzimidazol-2-yl-phenol derivatives (HL₁-HL₅) were prepared according to our reported procedures [14]. The iron(II) complexes were synthesized by treating the corresponding ligand with the methanol solution of FeCl₂·4H₂O. The color of iron(II) complexes was brown-orange or black grey and also, they had good yields (50-69%) with high purity. These complexes are stable in both solution and solid state. The analytical data and physical properties of the ligands and their complexes are summarized in table S1. The formation of complexes was further supported by the results of FT-IR and UV-vis spectra, ICP and elemental analysis (C, H and N). Elemental analysis showed the general formula for complexes **C1** and **C2** were as K₂[Fe(L₁)₂Cl₂]·4H₂O and K₂[Fe(L₂)₂Cl₂]·H₂O, respectively, while in complexes **C3**, **C4** and **C5**, it was obtained as K₂[Fe(L₃)₂Cl₂], [Fe(L₄)₂] and K₂[Fe(L₅)₂Cl₂]·2(CH₃OH), respectively. During the procedure, it was difficult to achieve the single-crystals of all complexes, although the complexes were prepared in several different solvents. Besides, the few obtained crystals were not suitable for X-ray diffraction, as well. Therefore, it was decided to determine the molecular structures of complexes by using DFT calculations. Theoretical calculations involving geometry optimization, vibrational frequencies, stability of the compounds, as well as the various bond lengths and angles generated from the optimized structure was also performed on the ligands and complexes which will be discussed further in the following sections.

3.1. Geometrical parameters of the ligands and complexes

The optimized geometry of HL₅ is shown in figure 1 as a representative structure. The various bond lengths and angles generated from the structures of the optimized ligand (HL₅) and complex (**C5**) are obtained. They showed good similarity with the X-ray structural investigations of analogous ligands and complexes reported [26-29]. The computed bond lengths for HL₅ O(1)-C(6), O(1)-H(24), N(3)-C(7), N(3)-C(9), N(8)-C(7), N(8)-C(2), are 1.34, 0.99, 1.38, 1.34, 1.32 and 1.38 Å, respectively. The computed bond angles, C(6)-O(1)-H(24), C(7)-N(3)-C(9), C(7)-N(8)-C(2) and N(8)-C(7)-N(3) in HL₅ are 108.47°, 107.70°, 106.49°, 111.20°, respectively.

The computed bond lengths Fe(49)-O(1), Fe(49)-O(7), Fe(49)-N(8), Fe(49)-N(31) (30), Fe(49)-Cl(47) and Fe(49)-Cl(48) in complex **C5** are 2.11, 2.11, 2.23, 2.23, 2.62 and 2.60 Å, respectively. The computed bond angles in complex **C5**, such as N(8)-Fe(49)-O(1) (=97.95°), N(8)-Fe(49)-O(7) (=82.11°), N(8)-Fe(49)-Cl(47) (=88.65°), N(8)-Fe(49)-Cl(48) (=91.33°), N(8)-Fe(49)-N(31) (=177.32°), N(31)-Fe(49)-O(1) (=82.11°), N(31)-Fe(49)-O(7) (=97.94°), N(31)-Fe(49)-Cl(47) (=88.66°), N(31)-Fe(49)-Cl(48) (=91.33°), O(1)-Fe(49)-O(7) (=177.27°), O(1)-Fe(49)-Cl(47) (=91.36°), O(1)-Fe(49)-Cl(48) (=88.63°), O(7)-Fe(49)-Cl(47) (=91.35°), O(7)-Fe(49)-Cl(48) (=88.63°) and Cl(47)-Fe(49)-Cl(48) (=179.99°) suggest octahedral structure. The optimized structure of **C5** is shown in figure 2.

3.2. FT-IR spectroscopy of the ligands and complexes

Vibrational properties of the ligands and complexes have been done by using the DFT calculations and FT-IR instrument. The striking bands in the FT-IR spectra of the complexes are given in table S2. As an example, the measured and calculated FT-IR spectra of the HL₅ ligand and its related complex, *i.e.* **C5**, are compared in figures 3(a,b) and 4(a,b), respectively. In our earlier work [14], vibration frequencies of the ligands HL₁₋₅ were noted and were in agreement with the theoretical calculations. Considering their FT-IR spectra, the vibrational modes of N-H (~1479 cm⁻¹), C=C (~1558 cm⁻¹), C=N (~1631 cm⁻¹) and C-O (~1259 cm⁻¹) bonds in **C1-C5** shifted to lower wavenumbers [30], in comparison with their corresponding free ligands HL₁₋₅ ($\nu(\text{N-H})$: ~1490 cm⁻¹, $\nu(\text{C=C})$: ~1591 cm⁻¹, $\nu(\text{C=N})$: ~1637 cm⁻¹ [31] and $\nu(\text{C-O})$: ~1298 cm⁻¹).

The vibrational frequency of N-H, C=C, C=N, C-O in predicted theoretical spectra of the complexes were calculated at ~1480 cm⁻¹, ~1552, ~1633 and ~1255 cm⁻¹, respectively. In the FT-IR spectra of complexes **C1-C5**, the imine nitrogen coordination could also be confirmed by appearance of a weak band located at the low wavenumber of (~426 cm⁻¹) which may belong to (Fe-N) [32, 33]. In high wavenumber region, bands at 2854-3184 cm⁻¹ are attributed to the stretching vibrations of aromatic C-H for complexes **C1-C5** [34, 35], and the corresponding peak in theoretical spectra were calculated at the range of 3001-3163 cm⁻¹. The sharp or medium bands in the complexes in the range of ~750-968 cm⁻¹ are due to the out-of-plane deformation bands for the aromatic C-H [36]. In complexes **C1-C5**, deprotonation and subsequent involvement of the phenoxy group in metal coordination could also be supported by the

appearance of new peaks at a lower wavenumber of (~ 461 , ~ 549 cm^{-1}) region assignable to (Fe-O). These results are in accord with the theoretical calculations.

The experimental and calculated FT-IR spectra of ligands and their complexes showed good agreement in terms of their peak frequencies, band intensities, and the shapes of the bands.

3.3. Electronic absorption spectra of the complexes

The UV-vis spectra were recorded from 200 to 800 nm in DMSO. UV-vis spectral data of HL₁₋₅ ligands were noted in our previous work [14]. The observed bands at lower wavelength bands (210-300 nm) correspond to $\pi \rightarrow \pi^*$ transitions of the aromatic rings. The bands in the range of 310-360 nm are due to $n \rightarrow \pi^*$ transitions [31]. The electronic spectra of complexes **C1-C5** show a broad band at 510, 480, 500 and 504 nm, respectively, which may be assigned to ${}^5T_{2g}(\text{D}) \rightarrow {}^5E_g(\text{D})$ transition. They are characteristic for high-spin octahedral geometry for **C1-C3** and **C5**. In the electronic spectrum of **C4**, there is a band at 510 nm that may be due to the ${}^5E(\text{D}) \rightarrow {}^5T_2(\text{D})$ transition [37, 38]. This characteristic is related to distorted tetrahedral geometry.

3.4. NMR spectra of the ligands

${}^1\text{H}$ -NMR spectra data of the ligands and the assignments of the peaks were reported in our previous work [14]. For example, the ${}^1\text{H}$ NMR spectra of HL₃, HL₄ and HL₅ ligands showed only a single broad band for the OH and the amine NH protons (13.14, 12.5 and 13.11 ppm for HL₃, HL₄ and HL₅, respectively). This combination is because of intramolecular hydrogen bonding between the O-H hydrogen and the C=N nitrogen atoms [39]. The ligands HL₁ and HL₂ gave two singlets for OH and NH protons (13.07 and 9.44 ppm for HL₁, 13.26 and 12.76 ppm for HL₂, respectively). In the ${}^1\text{H}$ -NMR spectra of HL₃ (including one methyl group) and HL₅ (including two methyl groups), a singlet was observed at 2.42 and 2.32 ppm, respectively. Position of protons and the assignments of the peaks in benzimidazole moiety and phenolic ring moiety in ligands HL₁₋₅ are various, due to the different functional groups in the benzimidazole ring. As our previous report, the chemical shift values of H1, H3 and H4 protons of HL₂ (having one chloro-substituent at the 5-position on the benzimidazole ring) were at 7.64, 8.04 and 7.37 ppm, and of HL₄ ligand (having two chloro-substituents at the 5,6-positions on the benzimidazole ring) were at 7.87, 8.05 and 7.38 ppm, respectively. Also, the chemical shift values of H1, H3 and H4 protons of HL₃ ligand (having one methyl substituent at the 5-position

on the benzimidazole ring) were at 7.43, 8.03 and 7.35 ppm, and in the HL₅ ligand (having two methyl substituents at the 5, 6-positions on the benzimidazole ring) were 7.40, 8.00 and 7.33 ppm, respectively. It is known that the chloro groups, electron withdrawing, on aromatic ring move the resonance of the H1, H3 and H4 protons downfield, while the methyl groups, electron donating, on ring move the resonance of these protons upfield. ¹H-NMR spectra of the ligands are shown in figure S1.

As already mentioned, in the ¹³C-NMR spectra of the synthesized ligands HL₁₋₅ (figure S2), there are signals around 157.71-158.98 and 150.83-153.77 ppm for carbon atoms bonded to the hydroxyl oxygen atom and imidazole C=N carbon atom, respectively. In the ¹³C-NMR spectra of HL₁₋₅, the observed signal around 132 ppm is assigned to C8 and C13 carbon atoms. Also the carbon atoms bonded to the chloro- and/or methyl- groups appear in the range of 125-133 ppm. The other signals belong to the benzimidazole benzene and phenol rings carbon atoms.

In our earlier work, ¹H- and ¹³C-NMR chemical shift calculations of HL₁₋₅ ligands were performed using the same functional and basis set as used for geometry optimizations. The results showed extreme agreement between experimental and computed chemical shifts (table 1).

3.5. Theoretical calculation and stability

According to the DFT calculations, Fe(II) complexes **C1** (-3556 a.u.), **C2** (-4475 a.u.), **C3** (-3635 a.u.), **C4** (-4474 a.u.) and **C5** (-3713 a.u.) have lower energy values than HL₁₋₅ ligands (HL₁: -686 a.u., HL₂: -1146 a.u., HL₃: -726 a.u., HL₄: -1606 a.u., HL₅: -765 a.u.). These numbers prove that ligands and the complexes containing the chloro- derivatives have higher stability than the methyl- derivatives when compared to each other. According to the DFT calculations, HL₁, as a ligand, and **C1**, as a complex, have the lowest stability among the ligands and the complexes, the synthesized compounds, respectively. Also, it is observed that **C2**, with one chloro-substituent, is slightly more stable (total energy: -4475 a.u.) than **C4**, containing two chloro-substituents (-4474 a.u.) (figure 5) and this lower stability of **C4** (despite having two chloro atoms) is due to the absence of chloro atoms attached to Fe atom. According to the geometry optimization of the structure of **C4** with DFT calculations, Fe is located on a distorted tetrahedral center with the imine nitrogen and hydroxy oxygen atoms of benzimidazole moiety and phenol ring, respectively, and for **C1-C3** and **C5** structures Fe is located on a distorted

octahedral center with one imine nitrogen and the phenolate oxygen atom along with two chloride ions (molecular symmetry: D_{2h} for **C1-C3**, **C5** and C_{2v} for **C4** complexes).

3.6. Ethylene oligomerization

All the synthesized iron(II) complexes, when activated with diethylaluminum chloride (Et_2AlCl), show high catalytic activities for ethylene oligomerization with high selectivity for 1-butenes at 20 atm of ethylene pressure. Also, the distribution of oligomers does not follow Schulz-Flory rules. No oligomer with odd carbon number was found in the GC analysis [40]. The detailed results are summarized in table 2.

3.6.1. Ethylene oligomerization by iron(II) complexes C1-C5. It should be pointed out that the selectivity for linear α -olefins of oligomers was varied with the ligand environments. However, no unambiguous trend could be identified. The oligomers are only obtained and measured by GC. Iron(II) complexes were initially studied for their catalytic activities in ethylene oligomerization at 20 atm of ethylene pressure. The effects of the ligand environment were studied in the ethylene reactivity. All the synthesized iron(II) complexes, when activated with Et_2AlCl , display modest-to-high catalytic activities for ethylene oligomerization with high selectivity for α -olefins. Apart from **C1** complex ($R_1 = R_2 = H$), which generated dimer and trimer oligomeric products, **C2-C5** complexes generated only dimer as main oligomeric product. The detailed results are summarized in table 2. The variation of the R-substituent on the benzimidazole resulted in changes of the catalytic performance. Among iron catalysts, complex **C1** ($R_1 = R_2 = H$) showed the lowest catalytic activities and **C4** complex ($R_1 = R_2 = Cl$) showed the highest activity among their analogues. According to table 2 (entries 1-5), the oligomerization activities decreased in the order $C4 > C2 > C3 > C5 > C1$. Comparing the catalysts activity, it can be found that complexes **C2** and **C4** containing electron-withdrawing halogen groups showed high catalytic activity. On the contrary, relatively lower productivity was observed with the complexes bearing electron-donating alkyl groups such as complexes **C3** and **C5**, despite their good selectivity toward 1-butene. It can be concluded that the catalytic activities ascend with an increase in the number of Cl atoms in the ligand, probably ascribed to the electron-withdrawing nature of chlorine atom, which leads to increase of the electrophilic iron center and decrease of the electron density in the benzimidazole rings [41] as well as leads

to increased selectivity for α -olefins. It can be concluded that the d orbital of iron is almost empty and therefore it has strong bond with the ligand, which causes little space for ethylene coordination, and the ethylene monomer does not reach the active center well and the activity is reduced. For this reason, when electron-withdrawing Cl groups are placed on the ligand, it causes the electron density to drop around the metal and the ethylene monomer interacts easily with the active center and increases its activity. In versus, the methyl groups at the benzimidazole ring of complexes **C3** and **C5** may prevent the access of ethylene to the active center in the catalytic system, therefore resulting in the decrease of catalytic activity. Also, activity decrease can probably be attributed to the increasing nucleophilicity of the metal center with higher number of methyl groups on the phenyl ring, which weakens the interaction between the iron atom and the π -electrons of ethylene monomer and decreases the rate of ethylene insertion in the chain-growth steps [26]. Furthermore, incorporating an electron-donating methyl group on the benzimidazole rings might push more electrons to the iron atom, reduce the net charge on the iron center, and therefore, resulted in lower catalytic activity for ethylene oligomerization [42]. It is a general notion that decrease in the donor ability of the substituents, (*i.e.* increase in the electrophilicity of the metal center) should decrease the insertion barrier, thus, resulting in higher activity [43].

Briefly, iron catalysts generally produce ethylene dimer and have high selectivity for 1-butene, in other words, with higher catalytic activity, the content of C_4 is obviously increased, because β -hydrogen elimination was faster than ethylene propagation and the distribution of obtained oligomers did not resemble Schulz-Flory rules.

4. Conclusion

Fe(II) complexes containing 2-(2-hydroxyaryl)-1*H*-benzimidazole derivatives were synthesized and characterized. In conclusion, the structures of the compounds were verified by FT-IR, ^1H -, ^{13}C -NMR and UV-vis spectroscopy, ICP and elemental analysis. According to the DFT calculations, in all complexes, the ligands are coordinated bidentately *via* one imine nitrogen and the phenolate oxygen atoms. Furthermore, in all iron(II) complexes, the structure with four unpaired electrons had the minimum energy among other electronic structures which shows that the complexes were basically in high-spin mode. All the analytical and spectral data are consistent with theoretical calculations. These complexes could be easily activated and exhibited

good activities for ethylene oligomerization in the presence of Et₂AlCl as cocatalyst, even though the amount of cocatalyst was very small and the main products were 1-butenes of ethylene.

Supplementary material

Cartesian coordinates of all the species discussed in the text together with spectral data for the synthesized ligands are available free of charge via the Internet at the publisher's website.

Acknowledgement

This work was supported by Iran University of Science and Technology, Iran Polymer and Petrochemical Institute and Petrochemical Research & Technology Company. Naeimeh Bahri-Laleh thanks MOLNAC (www.molnac.unisa.it) for its computer facilities.

References

- [1] P. Hao, Y. Chen, T. Xiao, W.H. Sun. *J. Organomet. Chem.*, **695**, 90 (2010).
- [2] G.J.P. Britovsek, V.C. Gibson, S.J. McTavish, G.A. Solan, A.J.P. White, D.J. Williams, G.J.P. Britovsek, B.S. Kimberley, P.J. Maddox. *Chem. Commun.*, **1998**, 849 (1998).
- [3] G.J.P. Britovsek, S. Mastroianni, G.A. Solan, S.P.D. Baugh, C. Redshaw, V.C. Gibson, A.J.P. White, D.J. Williams, M.R.J. Elsegood. *Chem. Eur. J.*, **6**, 2221 (2000).
- [4] B.L. Small, M. Brookhart, A.M.A. Bennett. *J. Am. Chem. Soc.*, **120**, 4049 (1998).
- [5] L. Guo, C. Chen. *J. Sci. China Chem.*, **58**, 1663 (2015).
- [6] C. Li, H. Yu, Z. Lin, F.F. Wang, N. Zhang, J. Wang. *J. Coord Chem.*, **70**, 1303 (2017).
- [7] W.H. Sun, S. Zhang, W. Zuo. *C. R. Chimie*, **11**, 307 (2008).
- [8] L. Xiao, R. Gao, M. Zhang, Y. Li, X. Cao, W.H. Sun. *Organometallics*, **28**, 2225 (2009).
- [9] Y. Chen, P. Hao, W. Zuo, K. Gao, W.H. Sun. *J. Organomet. Chem.*, **693**, 1829 (2008).
- [10] C.Q. Li, F.F. Wang, R. Gao, P. Sun, N. Zhang, J. Wang. *Transition Met. Chem.*, **42**, 339 (2017).
- [11] N. Zhang, S. Wang, L. Song, C. Li, J. Wang. *Inorg. Chim. Acta*, **453**, 369 (2016).
- [12] Z.J. Yao, K. Li, J. Y. Zhang, Y. Wang, W. Deng. *Inorg. Chim. Acta*, **450**, 118 (2016).
- [13] O. Dayan, M. Tercan, N. Özdemir. *J. Mol. Struct.*, **1123**, 35 (2016).
- [14] M. Haghverdi, A. Tadjarodi, N. Bahri Laleh, M. Nekoomanesh Haghghi. *Appl. Organomet. Chem.*, **32**, aoc.4015 (2018).

- [15] C. Lee, W. Yang, R.G. Parr. *J. Phys. Res., Part B*, **37**, 785 (1988).
- [16] A.D. Becke. *J. Chem. Phys.*, **98**, 1372 (1993).
- [17] A. Schäfer, H. Horn, R. Ahlrichs. *J. Chem. Phys.*, **97**, 2571 (1992).
- [18] M.K.F. Nouri Ahangarani, N. Bahri Laleh, M. Nekoomanesh Haghghi. *Des. Monomers Polym.*, **19**, 394 (2016).
- [19] N. Bahri Laleh, A. Poater, L. Cavallo, S.A. Mirmohammadi. *Dalton Trans.*, **43**, 15143 (2014).
- [20] N. Bahri Laleh, M. Nekoomanesh Haghghi, S.A. Mirmohammadi. *J. Organomet. Chem.*, **719**, 74 (2012).
- [21] N. Bahri Laleh, L. Falivene, L. Cavallo. *Polyolefins J.*, **1**, 139 (2014).
- [22] A. Poater, L. Falivene, C.A. Urbina Blanco, S. Manzini, S.P. Nolan, L. Cavallo. *Dalton Trans.*, **42**, 7433 (2013).
- [23] M.J. Frisch, G.W. Trucks, H.B. Schlegel, Gaussian 09, Gaussian, Inc., Wallingford, CT (2009).
- [24] S. Kundu, S. Biswas, A. Sau Mondal, P. Roy, T. Kumar Mondal. *J. Mol. Struct.*, **1100**, 27 (2015).
- [25] M.M. Ibrahim, A.M.M. Ramadan, H.S. El Sheshtawy, M.A. Mohamed, M. Soliman, S. Imam. *J. Coord. Chem.*, **68**, 4296 (2015).
- [26] Q. Shi, S. Zhang, F. Chang, P. Hao, W.H. Sun. *C. R. Chimie*, **10**, 1200 (2007).
- [27] L.L. Han. *Acta Cryst. E*, **66**, 2047 (2010).
- [28] P. Hao, S. Zhang, W.H. Sun, Q. Shi, S. Adewuyi, X. Lu, P. Li. *Organometallics*, **26**, 2439 (2007).
- [29] X. Chen, L. Zhang, T. Liang, X. Hao, W.H. Sun. *C. R. Chimie*, **13**, 1450 (2010).
- [30] P. Saha, J. Prakash Naskar, A. Bhattacharya, R. Ganguly, B. Saha, S. Chowdhury. *J. Coord. Chem.*, **69**, 303 (2016).
- [31] A. Tavman, I. Boz, A. Seher Birtöksöz, A. Cinarli. *J. Coord. Chem.*, **63**, 1398 (2010).
- [32] S.S. Qian, X.L. Zhao, L.H. Pang, Z.L. You, H.L. Zhu. *J. Coord. Chem.*, **42**, 345 (2016).
- [33] M.M. Abd Elzaher. *Appl. Organomet. Chem.*, **18**, 149 (2004).
- [34] N. Sundaraganesan, C. Meganathan, B. Anand, C. Lapouge. *Spectrochim. Acta, Part A*, **66**, 773 (2007).

- [35] C.A. Téllez S., A.C. Costa Jr., M.A. Mondragón, G.B. Ferreira, O. Versiane, J.L. Rangel, G. Müller Lima, A.A. Martin. *Spectrochim. Acta, Part A*, **169**, 95 (2016).
- [36] A. Tavman, I. Boz, A. Seher Birteksöz. *Spectrochim. Acta, Part A*, **77**, 199 (2010).
- [37] A. Tavman, N.M. Agh-Atabay, A. Neshat, F. Guçin, B. Dulger, D. Hacıu. *Transition Met. Chem.*, **31**, 194 (2006).
- [38] A. Tavman, N.M. Agh-Atabay, S. Guner, F. Guçin, B. Dulger. *Transition Met. Chem.*, **32**, 172 (2007).
- [39] N. Sundaraganesan, B. Anand, F.F. Jian, P. Zhao. *Spectrochim. Acta, Part A*, **65**, 826 (2006).
- [40] X. Tang, W.H. Sun, T. Gao, J. Hou, J. Chen, W. Chen. *J. Organomet. Chem.*, **690**, 1570 (2005).
- [41] C. Görl, N. Beck, K. Kleiber, H.G. Alt. *J. Mol. Catal. A: Chem.*, **352**, 110 (2012).
- [42] M. Zhang, R. Gao, X. Hao, W.H. Sun. *J. Organomet. Chem.*, **693**, 3867 (2008).
- [43] X. Tang, D. Zhang, S. Jie, W.H. Sun, J. Chen. *J. Organomet. Chem.*, **690**, 3918 (2005).

Figure captions

Figure 1. Optimized structure of ligand HL₅ at B3LYP/TZVP level of theory.

Figure 2. Optimized structure of complex C5 at B3LYP/TZVP level of theory.

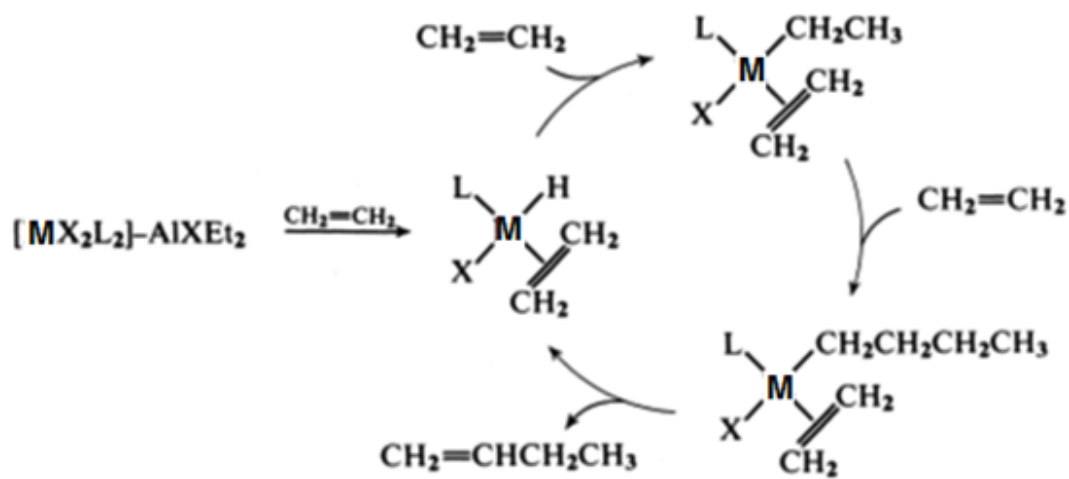
Figure 3. Comparison of (a) experimental FT-IR and (b) theoretical FT-IR calculated at B3LYP/TZVP level, spectra for HL₅.

Figure 4. Comparison of (a) experimental FT-IR and (b) theoretical FT-IR calculated at B3LYP/TZVP level, spectra for complex C5.

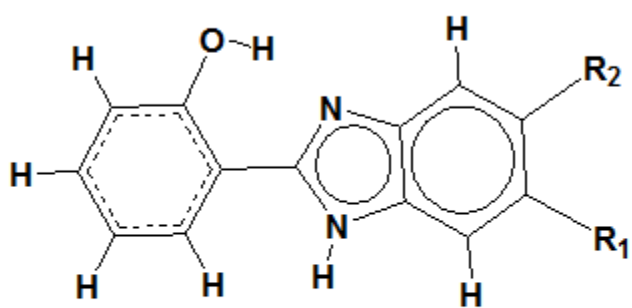
Figure 5. Optimized structure of complex C4 at B3.

Graphical abstract

10T



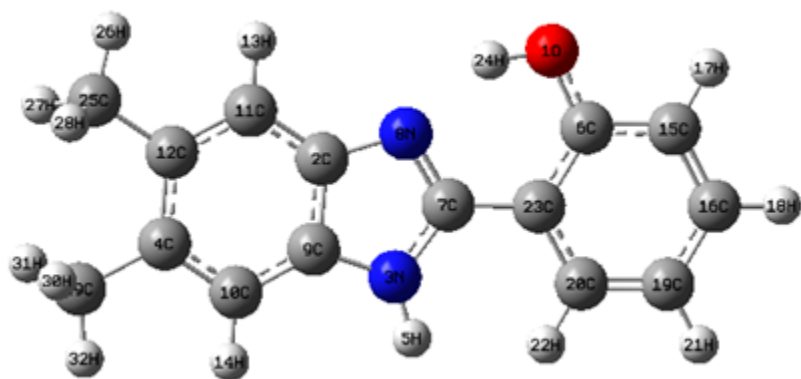
ACCEPTED



- HL₁: R₁ = R₂ = H
HL₂: R₁ = Cl, R₂ = H
HL₃: R₁ = CH₃, R₂ = H
HL₄: R₁ = R₂ = Cl
HL₅: R₁ = R₂ = CH₃

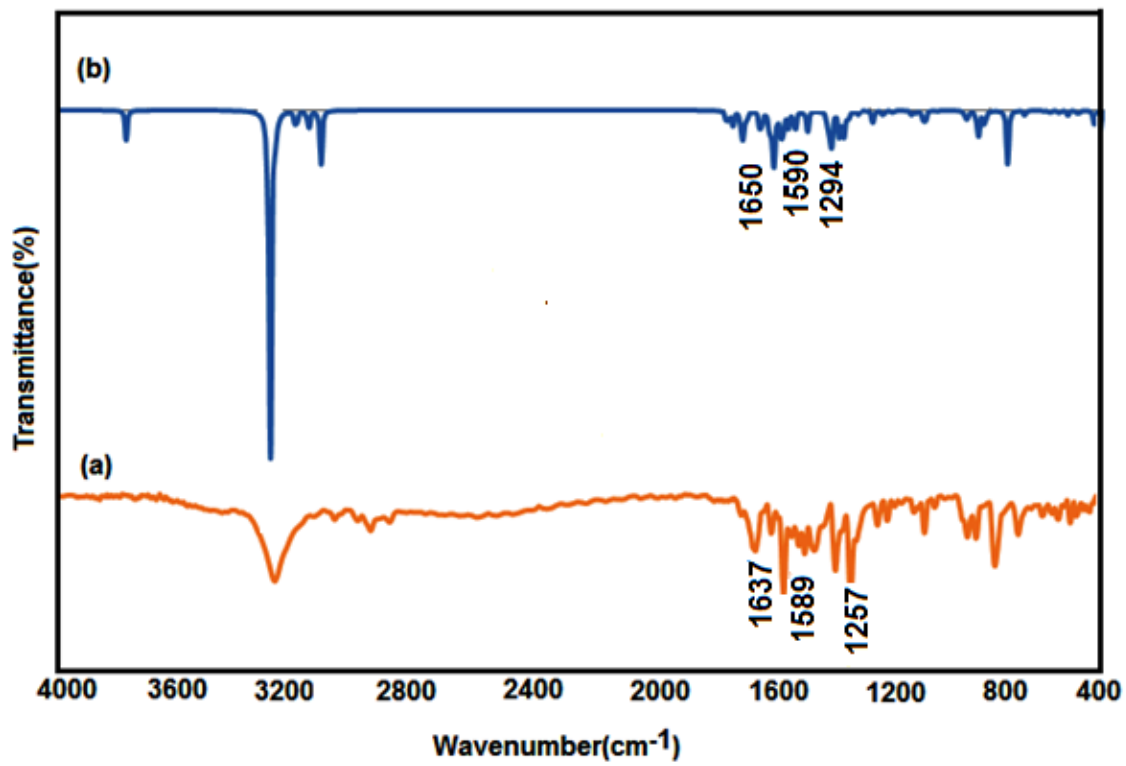
USCRIPT

ACCEPTED

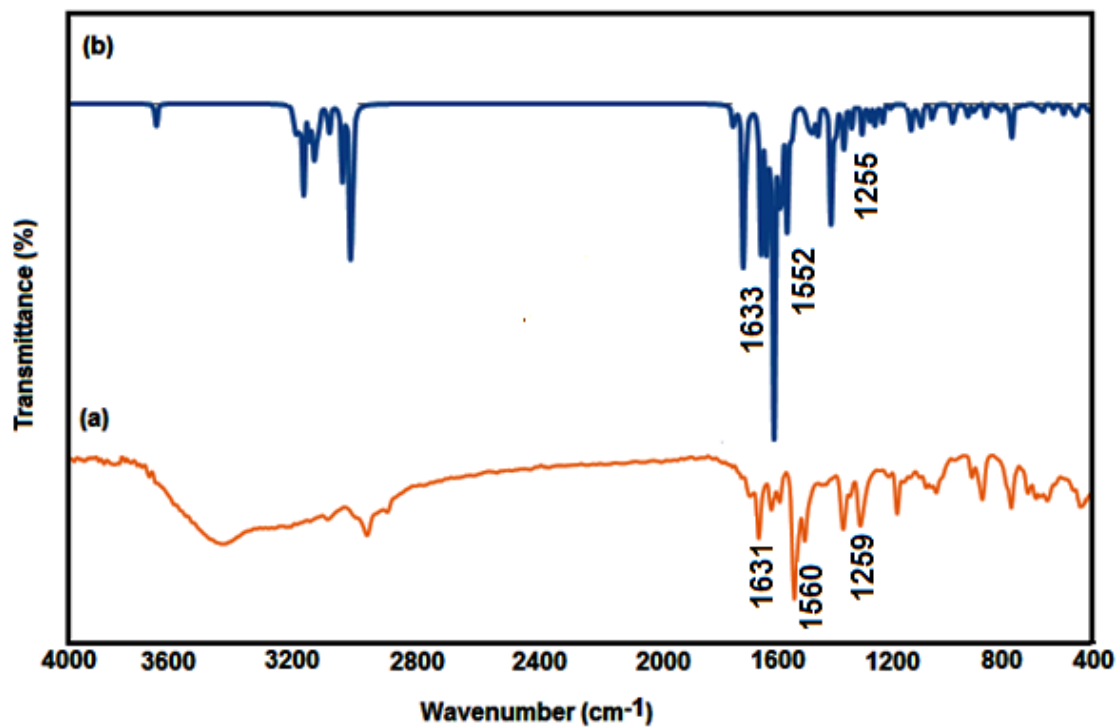


SCRIPT

ACCEPTED MANUSCRIPT



ACCEPTED



ACCEPTED

Table 1. Theoretical assignment of ^1H -NMR and ^{13}C -NMR data for the ligands optimized by B3LYP/TZVP level: the chemical shift values (δH , ppm).

Ligands	Proton assignment	^1H -NMR (Experimental)	^1H -NMR (Theoretical)	Carbon assignment	^{13}C -NMR (Experimental)	^{13}C -NMR (Theoretical)
HL ₁	NH	9.44	8.45	C=N	151.35	154.20
	OH	13.07	13.20	C-OH	158.98	167.80
HL ₂	NH	12.76	8.40	C=N	152.85	156.00
	OH	13.26	12.90	C-OH	157.87	168.00
HL ₃				C-Cl	126.59	143.00
	NH	13.14	8.35	C=N	151.40	154.00
	OH	13.14	13.20	C-OH	157.98	167.00
	CH ₃	2.42	2.50	C-CH ₃	131.54	137.00
HL ₄				-CH ₃	21.29	21.00
	NH	12.50	8.25	C=N	153.77	156.00
	OH	12.50	12.62	C-OH	157.71	167.70
				C-Cl	124.99	140.50
HL ₅	NH	13.11	8.30	C=N	150.83	153.80
	OH	13.11	13.20	C-OH	157.92	167.00
	CH ₃	2.32	2.35	C-CH ₃	131.31	136.00
			-CH ₃	19.96	20.10	

Table 2. Results of ethylene oligomerization with **C1–C5**/ Et₂AlCl^a.

Entry	Precatalyst	Yield (g)	Activity ^b	Oligomer distribution ^c (%)			
				C ₄	C ₆	α-C ₄	α-C ₆
1	C1	1.72	344	93.11	6.89	91.91	100
2	C2	8.32	1664	100	-	62.16	-
3	C3	8.20	1640	100	-	100	-
4	C4	8.43	1686	100	-	100	-
5	C5	8.13	1626	100	-	84.21	-

^a General conditions: 10 μmol precatalyst, 100 mL toluene as solvent, [Al]/[Fe] = 200, 20 atm of ethylene, reaction time 0.5 h, reaction temp. 30 °C. ^b In units of kg oligomers.mol⁻¹(Fe).h⁻¹. ^c Determined by GC. ΣC denotes the total amounts of oligomers.